Ductile Fracture of 7075-T651 Aluminum Alloy

Saeid Hadidi-Moud[1,a] , Seyed Farhad Hosseini[2,b]

[1] Department of mechanical engineering, The University of Birjand, Iran

[2] Department of mechanical engineering, Ferdowsi University of Mashhad, Iran

[a]Hadidi@um.ac.ir, s.hadidimoud@Birjand.ac.ir, [b] Farhad.ho67@gmail.com

Keywords: Ductile Fracture, GTN model, Calibrated Parameters, 7075-T651 Aluminum Alloy

Abstract. In this paper the capability of Gurson-Tvergaard-Needleman (or GTN) model in the prediction of ductile damage in 7075-T651 aluminum alloy is investigated. For this purpose, three types of specimens were tested: Standard tensile bars, Round notched bar (RNB) specimens and compact tension (C(T)) specimens. Standard tensile bar tests were used to obtain the mechanical properties of the material and to calibrate the independent parameters of GTN model. RNB and C(T) specimen test results were used for validation of the calibrated parameters. Finite element analyses were carried out using ABAQUS commercial software for two purposes; calibration of the GTN model parameters and validation of the model predictions. The comparison between the finite element analyses and the test results suggested that at least for this material the calibrated parameters can predict the failure conditions for both C(T) and RNB specimens.

Introduction

Exhibiting excellent mechanical properties has placed 7075 aluminum alloys amongst the widely used engineering materials in light weight structures especially in the aircraft and aerospace industry. Careful examinations of fractured surfaces of components made of this material using scan electron microscopy have revealed that under quasi static loading conditions, although a rather abrupt fracture incident is often observed, the mechanism of fracture is mainly ductile and failure takes place through nucleation, growth and coalescence of micro-voids [1]. More specifically the ductility of the alloy is typically governed by the nucleation of the primary voids [2]. The secondary void nucleation and growth also occurs at smaller sized particles. Finally void coalescence takes place by the joining of primary and secondary voids. Although the major cause of damage is due to primary voids but the nucleation and growth from secondary voids would reduce the ductility. Therefore, due to the leading role of these features in description of fracture it is anticipated that a Gurson-Tvergaard-Needleman (GTN) model [3] should provide an appropriate explanation of the fracture event in great details.

Implementation of GTN model in the finite element program, ABAQUS, provides a numerical way to identify its parameters. The process of calibration of parameters for the 7075-T651 aluminum alloy is discussed later in this paper. Finally the RNB and C(T) test results are used for validation of the calibrated parameters for this material.

The GTN model

In 1977 Gurson [4] suggested a way to reach an appropriate yield surface for a voided material. The Garson's yield function described by the following equation:

$$\Phi = \left(\frac{\sigma_{eq}}{\sigma_y}\right)^2 + 2f.cosh\left(\frac{3\sigma_m}{2\sigma_y}\right) - 1 - f^2 = 0 \qquad (1)$$

where σ_{eq} is the equivalent Von Mises stress, σ_m and σ_y refer to the mean stress the yield stress of the material respectively. Also f is the void volume fraction which is defined as the ratio of the total volume of all cavities to the volume of the body. Considering the interaction between adjacent holes, Tvergaard [5] introduced q_1 and q_2 parameters to modify the yield surface. Furthermore, Tvergaard and Needleman [3] substituted the void volume fraction f in the original equation by a modified void volume fraction f^* in order to account for the loss of load bearing capacity due to the void coalescence. Considering the above modifications, the equation (1) changes to:

$$\Phi = \left(\frac{\sigma_{eq}}{\sigma_y}\right)^2 + 2q_1 f.cosh\left(\frac{3q_2\sigma_m}{2\sigma_y}\right) - 1 - (q_1 f^2) = 0 \tag{2}$$

and the function f^* is given by:

$$f^*(f) = \begin{cases} f & f \le f_c \\ f_c + \frac{f_u^* - f_c}{f_f - f_c}(f - f_c) & f > f_c \end{cases} \tag{3}$$

wheref_c and f_f are the critical void volume fraction and the void volume fraction at total failure respectively and f_u sets to $1/q_1$, so the modified void volume fraction f^* corresponds to the void volume fraction f unless the critical porosity f_c is exceeded.
It should be pointed out that for $q_1 = q_2 = 1$, the equation 2 reduces to equation 1 and if f is set to zero, the material would be without any porosity and the Garson's yield function reduces to the Von Mises yield function.
Since change in porosity of the material is due to the combination of growth and nucleation, the evolution of void volume fraction is given by:

$$\dot{f} = \dot{f}_{growth} + \dot{f}_{nucleation} \tag{4}$$

where $\dot{f}_{growth}$ is the change due to the growth of existing voids and $\dot{f}_{nucleation}$ is the change due to the nucleation of new voids. The law of conservation of mass requires:

$$\dot{f}_{growth} = (1-f)\dot{\varepsilon}^p : I \tag{5}$$

where $\dot{\varepsilon}_e^{pl}$ is the equivalent plastic strain. Nucleation is assumed to be strain controlled and normally distributed in the following manner:

$$\dot{f}_{nucleation} = A\dot{\varepsilon}_e^p \tag{6}$$

Where

$$A = \frac{f_N}{S_N\sqrt{2\pi}} \exp\left\{-\frac{1}{2}\left[\frac{\varepsilon_e^p - \varepsilon_N}{S_N}\right]^2\right\} \tag{7}$$

Nucleation strain is normally distributed with mean value ε_N and standard deviation S_N as parameters. f_N is the maximum void volume fraction of nucleated voids.
The explained GTN model has 8 independent parameters (ε_N, S_N, f_N, f_c, f_f, f_0, $q_1$and q_2) which should be calibrated by means of comparing the experimental load-displacement curve obtained from standard test specimens with the simulated load-displacement results. A detailed explanation of this procedure is presented in the next section.

The experimental program

Material. To obtain the yield properties of the material and calibrate the parameters of the GTN model, tensile tests were carried out for three standard tensile bars using ASTM B551 standard test method for aluminum bars [6]. The results obtained from the three specimens were almost identical. Figure 1 shows the resulted true stress- true strain curve.

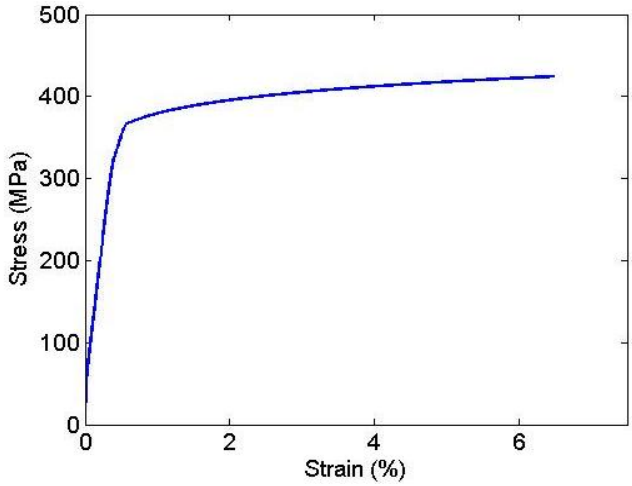

Fig. 1. True stress - True strain curve

Using figure 1, the mechanical properties of the material were obtained as shown in table 1.

Table1. Mechanical properties of material

E[Gpa]	S_y[Mpa]	S_{ut}[Mpa]	Fracture strain[%]
71	363	420	6.23

The load-displacement data obtained from these standard tensile tests was then used to calibrate the GTN model parameters through comparison with the FE analysis results.

RNB and C(T) Testing. Because of the need to validate our predictions, tests were carried out on RNB and C(T) specimens. Table 2 shows geometrical details of the RNB specimens.

Table2. The specifications of RNB specimens

Specimen name	D[mm]	d (net section) [mm]	Radius[mm]	Number of specimens
9-0.15	18	9	0.15	3
13-0.15	18	13	0.15	3
9-1.1	18	9	1.1	3
13-1.1	18	13	1.1	3
9-4.4	18	9	4.4	3
13-4.4	18	13	4.4	3

As typical examples, details of two RNB specimens, 13-0.15 and 13-4.4 are shown in figure 2 and the load-displacement results for RNB9-1.1 specimens are plotted in figure 3.

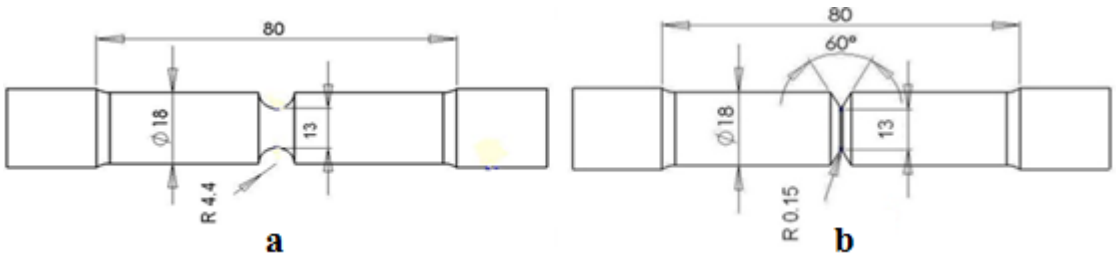

Fig.2. A complete description of two RNB specimens: (a) 13-4.4 and (b) 13-0.15

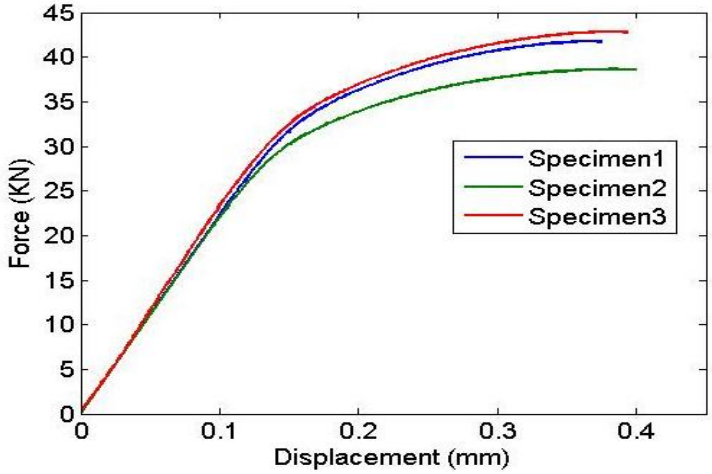

Fig.3. Load-displacement curves of RNB 9-1.1 specimens

Moreover, three identical CT specimens were tested using ASTM E399 standard with w=13 mm and $\frac{a}{w}$= 0.5 [6]. Figure 4 displays the load displacement curves obtained from CT testing. A Zwick testing machine was used for all experiments and specimens were loaded under displacement controlled loading at a constant rate of 1 mm/min.

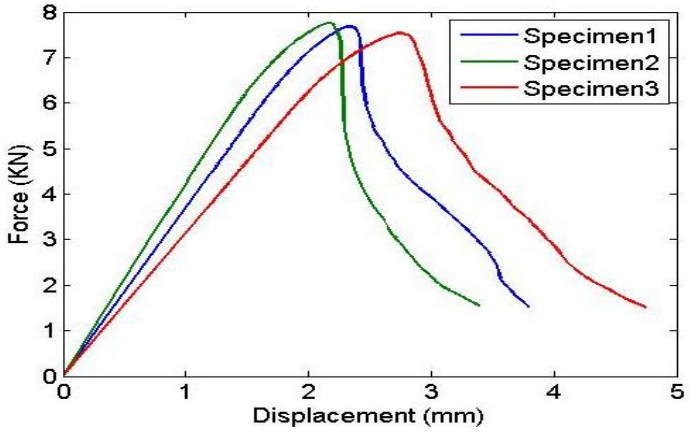

Fig.4. Load-displacement curves of C(T) specimens

The parameter used to compare the experimental findings with the FE results was “displacement at failure”. The values of this parameter for all RNB and C(T) specimens are listed in table 3.

Table 3. The values of displacements at total failure

Specimen name	Displacement at failure [mm]		
	Specimen 1	Specimen 2	Specimen 3
9-0.15	0.1907	0.2025	0.2159
13-0.15	0.3517	0.3656	0.4127
9-1.1	0.3746	0.3992	0.4144
13-1.1	0.5534	0.4622	0.5184
9-4.4	0.5580	0.4983	0.5334
13-4.4	0.8447	1.0759	1.0915
CT	2.2	2.35	2.8

FE Analyses

Elastic-Plastic finite element damage analyses based on GTN model were undertaken for the standard tensile bars. ABAQUS version 6.9 was used for all FE simulations. Axial symmetry conditions of RNB specimens allowed the use of axisymmetric meshes for standard tensile bars. The preliminary GTN parameters chosen from literature [7] were considered as initial estimates for the material model and were changed based on a step by step improvement procedure in order to get the best fit between the experimental load-displacement curve and simulated load-displacement curve. The generated axisymmetric FE model of the standard tensile bar is shown in figure 5(a). Figure 5(b) displays the best fit between the simulated and experimental curves using the final calibrated GTN parameters listed in table 4.

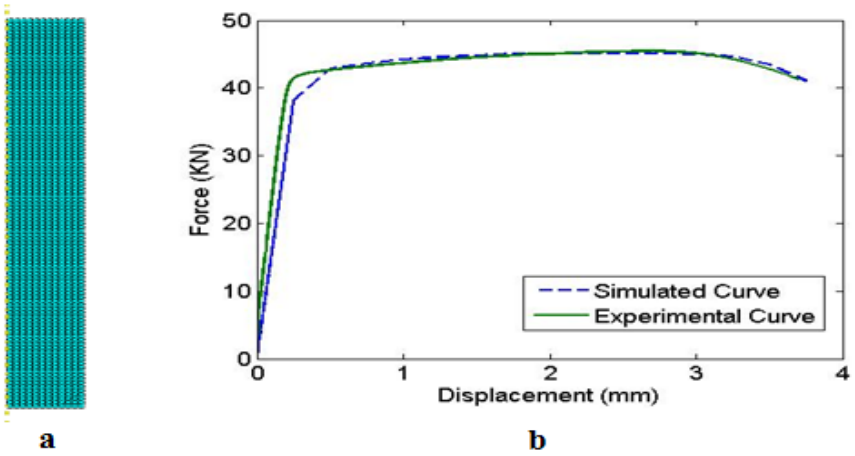

Fig.5. (a) Axisymmetric model of standard tensile bar and (b) The best fit between FE and experimental load-displacement curves

Table 4. Calibrated parameters of GTN model

Calibrated parameters	ε_N	S_N	f_N	f_c	f_f	f_0	q_1	q_2
	0.2	0.075	0.04	0.01	0.2	0.0085	1.5	1

It should be noted that since the calibrated parameters are empirical no unique set of parameters can be claimed [8].

Now, for validation purposes we apply the set of calibrated parameters to RNB and CT models in order to find out the displacement loads at failure. The findings were compared with the test results shown in table 3. The mesh size in validation specimens should be refined properly. This is important because the distance between the centers of two adjacent meshes is considered to be the distance between the two adjacent voids. It is crucial that the mesh size in RNB and CT models should be almost the same as that of standard tensile bar model which is already used in the calibration procedure. The condition of fracture for the RNB models is the loss of load carrying capacity of all elements at the net section area. This condition for CT model considered to be the loss of load carrying capacity of all elements at the crack front region. Figures 6(a) and

6(b) show the failure conditions for 13-0.15 RNB model and CT model respectively. Table 5 shows the simulated failure displacements of RNB and CT specimens. The test results are listed again in this table for comparison.

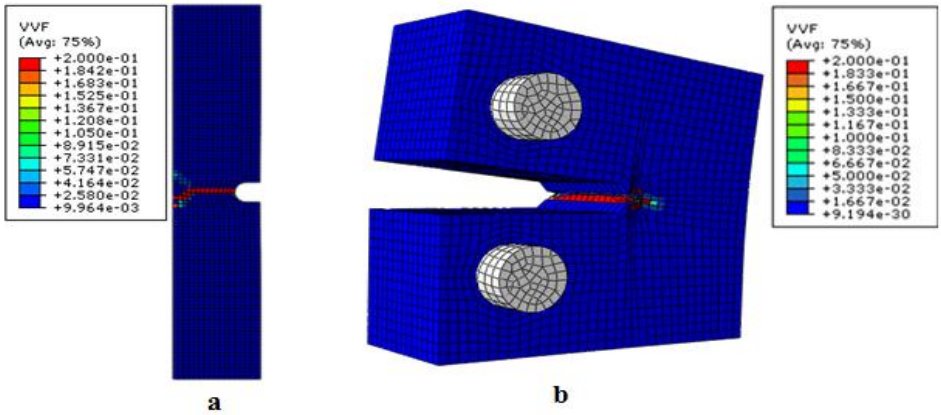

Fig.6. Fracture conditions (a) 13-4.4 specimen and (b) CT specimen

Table 5. Comparison between simulation and experimental displacements at fracture

Specimen name	Displacement at failure [mm]			
	Specimen 1	Specimen 2	Specimen 3	Simulation
9-0.15	0.1907	0.2025	0.2159	0.2300
13-0.15	0.3517	0.3656	0.4127	0.3826
9-1.1	0.3746	0.3992	0.4144	0.3890
13-1.1	0.5534	0.4622	0.5184	0.5398
9-4.4	0.5580	0.4983	0.5334	0.4535
13-4.4	0.8447	1.0759	1.0915	0.9405
CT	2.2	2.35	2.8	1.75

Results

The results shown in table 5 suggest that for the case of RNB specimens, the ductile damage prediction of GTN model for 7075-T651 aluminum alloy is great. However, the damage prediction for CT specimens seems to be conservative. For CT specimens, the use of special fixtures for the tests would influence the load point displacements. It is therefore anticipated that the use of CMOD parameter instead of displacement, would lead to more appropriate results. Overall, it may be concluded that the GTN model can be used as a suitable modeling tool in the prediction of ductile damage of 7075-T651 aluminum alloy.

References

[1] J. B. Jordon et. al.: *Damage characterization and modeling of a 7075-T651 aluminum plate*, Materials science and engineering A, Vol. 527 (2009), p. 169-178

[2] D. Fabregue, T. Pardoen: *A constitutive model for elastoplastic solids and secondary voids*, J. Mech. Phys. Solids, Vol. 56 (2008), p.719–741.

[3] Tvergaard V, Needlemann A.: *Analysis of the cup-cone fracture in a round tensile bar*, Acta Metall.,Vol. 32(1984), p. 57–69

[4] Gurson AL.: *Continuum theory of ductile rupture by void nucleation and growth: part I – yield criteria and flow rules for porous ductile media*, J Engng Mater Tech,(1977), p. 2–15

[5] Tvergaard V: *On localization in ductile materials containing spherical voids*, Int. J.Fract., Vol.18 (1982), p. 37–52

[6] Annual Book of ASTM Standard, ASTM (1997)

[7] Chang-Kyun, O. et al: A *Phenomenological Model of Ductile Fracture for API X65 Steel*, Internatinal Journal of Mechanical Science, Vol. 49 (2007), p. 1399-1412

[8] N. Benseddiq, A. Imad: *A ductile fracture analysis using a local damage model*, International Journal of Pressure Vessels and Piping, Vol. 85 (2008), p. 219–227